A Tool for the Optimization of Vertiport Locations for Urban and Suburban Passenger Transportation

Alejandro Montoya Santamaría, Miguel Baena Botana
Nommon Solutions and Technologies
Madrid, Spain

***Abstract*—Innovative Air Mobility (IAM), depends critically on the strategic placement of vertiports to enable safe and efficient operations. This paper presents a Hub Location Problem (HLP) framework for passenger vertiport siting that integrates demand estimation, operational conditions, and cost structures. Potential demand for the IAM air taxi is derived from mobile network data. Demand for taxi is estimated using logistic regression, with the likelihood of taxi passengers shifting to air taxis being calculated based on socioeconomic profiles and travel times. A case study in the Madrid region illustrates the ability of the framework to capture realistic demand and infrastructure requirements, offering a holistic and data-driven approach to the planning of IAM networks. A sensitivity analysis of the model is performed, showing that the selected locations are consistent in moderate user adoption scenarios, but change significantly when considering very high or very low adoption scenarios.**

***Keywords*—Vertiports, Innovative Air Mobility, Location Optimization, Hub Location Problem**

I. Introduction

In recent years, the aviation industry has transformed significantly due to advancements in electric Vertical take-off and landing (eVTOL) technology [1]. These developments are paving the way for Innovative Air Mobility (IAM), which will impact aircraft design, air traffic management (ATM), and multimodal transportation, creating new opportunities. However, successful IAM implementation depends on ground infrastructure that ensures safe operations in densely populated areas [2]. A primary challenge is the lack of suitable landing sites, or vertiports. Even if eVTOLs were certified today, cities do not have enough take-off and landing sites for fleet-scale operations [3]. Studies show that infrastructure is the most significant hurdle for IAM [2] [4].

Selecting vertiport locations is critical for establishing an efficient IAM system. Vertiport planning affects IAM performance, as it is the foundational infrastructure for operations [5]. In the field of passenger transportation, various approaches have been taken. Some focus on improving airport accessibility by creating vertiport networks near airports for multi-modal journeys [6]; others analyze urban mobility patterns to assess where air mobility can meet transportation needs [7]; and some contributions adopt a comprehensive approach considering sociodemographic data, travel patterns, and urban planning [8].

Classical site optimization problems can define a region's vertiport network. Mandatory Covering Problems (MCP) must satisfy all existing demand. Maximal Coverage Location Problems (MCLP) [9] address cases with limited supply. The Hub Location Problem (HLP) is common in logistics [10] [11], serving as points for consolidating flows between origins and destinations [12]. The procedures to calculate model aspects vary significantly. Objective functions may include revenue linked to captured demand and non-monetary externalities like noise or time savings for passengers, often weighted as "medical costs associated with noise" or "passengers' value of time" to measure all effects uniformly.

Despite advancements, existing vertiport location selection approaches have limitations. Frameworks focusing solely on airport access may overlook urban point-to-point travel demand, limiting IAM services' reach. Approaches based on commuting patterns may miss emerging transportation needs. Some comprehensive contributions lack relevant variables such as dynamic population data, weather conditions, access management, infrastructure requirements, and environmental considerations. Last-mile delivery vertiport placement methods often lack detailed delivery demand and traffic pattern information, leading to suboptimal decisions. Identifying optimal vertiport locations requires a holistic approach integrating operational and design requirements with advanced data analysis techniques to optimize placement accurately.

This research presents an optimization tool for locating passenger vertiports, considering realistic demand, local weather, restricted areas (e.g., airports), energy supply costs, maintenance, building costs, and revenues for operators. Demand is based on origin-destination matrices from mobile network data, capturing all travel between zones. A logit model, trained with mobility surveys, estimates taxi trips in a region, accounting for socioeconomic factors and distances, representing potential demand. A choice model based on travel time identifies trips likely to shift to air taxi services. This approach enhances previous research by incorporating more factors influencing vertiport locations, providing a realistic assessment of this new mobility service's viability. Finally, a case study in the Madrid region demonstrates the potential of the model.

The paper is structured as follows: Section II details the assumptions and optimization model for locating vertiports for passengers and last-mile delivery. After that, Section III presents the case study, and the data sources and processing required to obtain the inputs for the optimization. Section IV presents and analyzes the main results from the Madrid case study. Finally, Section V summarizes the research outcomes and conclusions.

II. Methodology

A. Assumptions

Forecasting passenger demand for eVTOL aircraft involves making assumptions based on the industry's early development stage, regulatory frameworks, infrastructure, and market acceptance. Therefore, we make the following assumptions for the optimization tool:

- **On-Demand network:** we assume an on-demand air taxi service without fixed routes. Hence, passengers can travel between all possible vertiport pairs.
- **Taxi based potential demand:** it is assumed that the potential demand for air taxi is linked with the current demand for taxi or other private road transportation services. Future eVTOL passenger volumes are estimated through a market penetration approach, where it is assumed that a certain fraction of trips currently served by conventional taxi services could be substituted by air taxis once they become available.
- **Inelastic demand:** this assumption is grounded in the fact that initial users are likely to belong to higher socioeconomic segments, for whom price sensitivity is lower compared to the general population. For these groups, the value proposition of eVTOLs (time savings, convenience, etc.) outweighs the cost premium relative to conventional transport modes.
- **Discretized demand:** the demand is spatially grouped into a set of discrete nodes that serve as the origins and destinations.
- **Daily time resolution:** the optimization uses demand data for an entire day, variations in demand throughout a day are not taken into account.
- **Minimum IAM travel distance:** we assume a minimum travel distance below which no passengers are willing to use IAM.
- **Free-route Airspace with Restricted Areas:** we assume a free-route U-space, meaning that eVTOLs travel in straight lines between vertiports, unless that path intersects a restricted area, in which case the eVTOL will take the shortest possible path avoiding that area.

B. Mode Choice

Given the assumption that all potential demand for the Air Taxi IAM service comes from current taxi demand, a binary choice model is needed to calculate the probability of a user opting to use air taxi or road taxi. We apply a heuristic inspired by the work of UBER [3]. In this white paper, it is assumed that when a trip is over 60 % faster by air taxi, the user always selects the air taxi option, otherwise road taxi is selected. In this research a daily averaged time is considered, but this model would work with variations of car time travel along the day due to congestion, capturing the greater shift to eVTOL in those cases. Due to the uncertainty in travel time estimates caused by spatial discretization and modeling error, we instead use a continuous and smooth sigmoid function, which ensures that small changes in drone velocity do not result in significant changes in demand.

$$P_{A,kd} = \left(1 + e^{\frac{6}{\min(1-\mathrm{TTRP},\mathrm{TTRP})}\left(\frac{t_{A,kd}}{t_{car}} - \mathrm{TTRP}\right)}\right)^{-1}. \quad (1)$$

The value $P_{A,kd}$ represents the probability of using an eVTOL, based on a sigmoid-like transition model that maps the ratio between the actual time of arrival by eVTOL ($t_{A,kd}$) and the time required for that same trip by car (t_{car}). The eVTOL trip time includes the access time from the origin to the departure vertiport and egress time from the arrival vertiport to the destination. The function can be modified based on the Travel Time Ratio Parameter (TTRP). Lower TTRP values mean that passengers need a greater velocity advantage from air taxi to select it over road taxi.

C. Mathematical Model for IAM Network

Following work in the literature, the vertiport site selection is framed as an HLP [11] [13]. In this problem, given an Origin-Destination (OD) matrix for travel demand, the vertiports are chosen such as to maximize or minimize an objective function (cost, traffic flow, revenue, etc). This approach models trips as three stages: origin to vertiport, flight phase, and vertiport to destination. This allows the optimization to capture the multimodal nature that is expected for IAM transportation.

The problem is framed from the point of view of the vertiport operator, where the objective is to maximize the profit with a limited number of vertiports. The first constraint is to set the number of vertiports to be built to n_{vert}, as shown in Equation (2). Where N is the number of potential locations considered in the problem and y_k is the decision variable for vertiport construction. It is 1 if the site is selected and 0 otherwise.

$$\sum_{k \in N} y_k = n_{vert}, \quad z_k \leq y_k, \quad \forall k \in N. \quad (2)$$

Decision variable z_k, also binary, represents whether a vertihub has been built at the location. For this variable, the second constraint in Equation (2) holds. A vertihub is a larger vertiport which can handle more operations per day than a standard vertiport. For a vertihub to be built, the location must be already selected as a vertiport.

For each trip p, the access and exit vertiport have to be selected. This decision variable is x^p_{kd}, which represents the fraction of the total potential demand for trip p that goes through vertiports k and d. Hence, both k and d must be selected as vertiports if that trip were to be possible. This must hold true for all trips in the set P of trips in the OD matrix used for the potential demand. See Equation (3):

$$x^p_{kd} \leq y_k, \quad \forall k \in N, \forall d \in N, \forall p \in P. \quad (3)$$

Furthermore, the sum of the fractions of the demand for a trip cannot exceed 1,

$$\sum_{k \in N} \sum_{d \in N} x^p_{kd} \leq 1, \forall p \in P. \quad (4)$$

Finally, each vertiport has a maximum number of operations that it can support per day. Each operation carries a certain number of passengers which depends on the drone size and the assumed occupancy rate. We then obtain a constraint of maximum passengers per day, where the capacity is determined by the type of vertiport (standard or vertihub).

$$\sum_{p\in P}\sum_{d\in N} P^p_{A,kd}D^p x^p_{kd} + P^p_{A,kd}D^p x^p_{dk} \leq n_{A,pass}(C_v y_k + (C_h - C_v)z_k), \quad \forall k \in N. \tag{5}$$

Where $n_{A,pass}$ is the average number of passengers per drone for drone model A, D^p is the passenger demand for trip p, C_h is the maximum number of operations per day for a vertihub and C_v for a standard vertiport. The objective function for maximizing the profit for the vertiport operator is presented below,

$$\max \sum_{p\in P}\sum_{k\in N}\sum_{d\in N} f^p_{A,kd} w_{A,kd} P^p_{A,kd} D^p x^p_{kd} - \sum_{k\in N} V_k y_k + (H_k - V_k)z_k. \tag{6}$$

Where V_k are the accumulated costs for a vertiport and H_k for a vertihub. w_{kd} is the fraction of days where the route from vertiport k to vertiport d is possible due to favorable weather conditions. The term $f^p_{A,kd}$ is the income per passenger for the vertiport operator. We model this with three separate components,

$$f^p_{A,kd} = c_{prices}\left(\frac{f_{op}}{n_{A,pass}} + f_{pass} + \frac{f_e E^p_{A,kd}}{n_{A,pass}}\right). \tag{7}$$

In the first component f_{op} is the charge per operation, f_{pass} the charge per passenger, f_e the charge per [kW] of electricity used to charge the drone, with the electricity cost subtracted. $E^p_{A,kd}$ is the electricity consumed by the eVTOL and c_{prices} is a factor set by the user.

The calculation for the costs in [EUR/day] is the same for both vertiports and vertihubs:

$$V_k = \frac{1}{365.25}\left(n_{emp,v}\,\mathrm{SAL} + \mathrm{MAI}_v\right) + \frac{1}{365.25 T_a}\left(\mathrm{CON}_k + \mathrm{INF}_v + F_k S_v\right). \tag{8}$$

Where n_{emp} is the number of employees, SAL is the estimated average yearly salary of the employees, MAI is the estimated yearly maintenance costs, T_a is the payback time in years, CON_k is the connection cost at location k, INF is the construction and installation costs of the vertiport (including charging stations), F_k are the estimated floor purchase costs in [EUR / m^2] at location k and S_v is the surface area required for the vertiport. The values for n_{emp}, MAI, and INF are different for vertihubs, but the formula remains the same.

III. Implementation and Case Study

A. Potential Demand Estimation from MND OD Matrices

For the case study, we have selected the province of Madrid, Spain as the target area for the IAM network. To estimate the demand we use the daily OD matrices generated by Nommon using Mobile Network Data (MND) for the Ministry of Transport of Spain [14]. The spatial resolution of these matrices is district level, which can range from less than 1 [km] in urban areas to the order of 10 [km] in rural areas. We use 4 weeks of OD matrices, one week from each quarter of 2024, and filtered out trips below 10 [km], as we assume these are unlikely to be candidates for IAM. The OD matrices contain information on the sex, income and frequency of the trip. However, the mode of transport is not available.

Therefore, to estimate the demand for taxi we train a linear logistic regression model on the data from the 2018 Madrid mobility poll [15]. The model uses as features the following fields, which are present both on the OD matrices and the poll:

- Travel distance d [km]: the Euclidean distance between the origin and the destination of a trip.
- Income per capita I_{pc}[EUR]: the average income per capita in the district of residence of the passenger. If this is not known, instead the average of the income capita of the origin and destination districts are used.
- Whether the trip is frequent or not B_{nof} [-]: this variable is equal to 1 if the trip is not frequently taken by the passenger and 0 otherwise.

We use a linear logistic regression. For binary classification, the expression is as follows

$$P(y = 1 \mid \mathbf{x}) = \frac{1}{1 + \exp(-(\mathbf{w}^\top \mathbf{x} + b))}, \tag{9}$$

where $y = 1$ when the trip is in a taxi. $\mathbf{w}$ are the trainable weights of the model, b is the trainable bias, and $\mathbf{x}$ is the vector of features. The model is trained for 2000 iterations using the lbfgs solver using only trips above 5 [km], resulting in a log loss in the test set of 0.034. The logistic regression model is then applied to each row of the OD matrix to estimate the number of taxi trips.

1) Market Penetration as a Function of Income: The fraction of trips in the mobility poll that are in taxi increase significantly in higher income neighborhoods. However, it is expected that due to the high initial costs of IAM passenger transportation, this difference could be greater for air taxi. Furthermore, we consider that using the entirety of the demand for road taxi as the demand for IAM is likely optimistic. Therefore, we introduce a model parameter k_{max} with value between 0 and 1 that limits the maximum achievable market penetration of the model. However, the value is modified depending on the income level of the passenger, with higher market penetration values among higher income passengers. We model this after the market penetration of taxi among all mobility, as shown in Table I.

This is done by keeping the ratio of market penetration values of air taxi in the taxi market between income levels

TABLE I. PERCENTAGE OF TOTAL TRIPS IN TAXI BY INCOME LEVEL. TRIPS OF OVER 5 [KM] IN THE 2018 MADRID MOBILITY POLL.

Income level [EUR]	Total trips [-]	Taxi trips [%]
0-15000	17121	0.46
15000- 20000	29536	0.70
20000-25000	19777	0.93
$>$ 25000	3956	1.39

the same as those for taxi among transportation in general. To achieve this, we solve a linear system of equations,

$$\begin{aligned} N_1 k^1_{max} + N_2 k^2_{max} + ... + N_m k^m_{max} &= N k_{max}, \\ k^n_{max} &= \frac{f_n}{f_{n+1}} k^{n+1}_{max}, \quad n = 1, ..., m-1. \end{aligned} \tag{10}$$

Where N_m is the total number of taxi trips of passengers in the income level m, N is the total number of taxi trips, f_m is the fraction of total trips of passengers in income level m that are in taxi and k^m_{max} is the maximum possible market penetration of air taxis within the taxi market among passengers in income level m. Finally, the rows with the same origin and destination pair p are grouped into a single row, and the number of trips is added to obtain the number of potential IAM daily passengers for p:

$$\begin{aligned} D^p &= \sum_{i \in \mathcal{I}} k^m_{max,i} \mathcal{D}_i P(y = 1 \mid \mathbf{x_i}), \\ \mathcal{I} &= \{i \mid \text{ODpair}_i = p\}. \end{aligned} \tag{11}$$

Where $\mathcal{D}_i$ is the number of total passengers in the ith row of the OD matrix.

B. IAM Travel Time Estimation

Since we assume a free-route airspace, we calculate the travel time based on the shortest distance between the access and egress vertiports, accounting for restricted areas. The restricted areas are modeled as polygons, based on which a baseline graph is created, where the nodes are the vertices of the polygons and the edges are all the straight line connections between vertices that do not intersect a polygon. Then, for each route we add the access and egress vertiports as two additional nodes and add all edges to other vertices which do not intersect any polygons. After that, the minimum distance between the two vertiports is calculated using the A* algorithm [16], with the weight of the edges being the Euclidean distance.

Once the distance d_{kd} between access vertiport k and egress vertiport d is calculated, we calculate the travel time $t_{A,kd}$ as shown in Equation (12):

$$t_{A,kd} = t_{delay} + 60 \frac{d_{kd}}{v_A}. \tag{12}$$

Where v_A is the cruise speed of drone A in [km/h] and t_{delay} [min] is the added time to account for security check, boarding and exiting the aircraft, and the take-off and landing phases.

C. Car Travel Time Estimation

We estimate travel time by car for any trip between any of the origins and destinations considered in the Madrid area by creating a surrogate model of an online navigation tool, Mapbox [17]. This tool has an API which allows for the estimation of the travel time by car between two different locations, accounting for speed limits, as well as the typical traffic in the area. This tool is sampled with a set of origins and destinations in the region of interest to create a dataset of travel times associated to OD pairs. After that, we perform a symbolic regression to find a function for travel time based on the following variables:

- d [km]: euclidean distance between the origin and destination.
- r_1 [km]: euclidean distance from origin to traffic center.
- r_2 [km]: euclidean distance from destination to traffic center.

We define the traffic center as the coordinate in the area of interest with the highest population residing within a 5 [km] radius. From these variables, we create a library of candidate functions that we used as features, following the approach presented by Schmelzer et al. [18]. Then, a linear regression is performed to find the associated coefficients of the following function for travel time in minutes in Madrid:

$$\begin{aligned} t_{car} = &- 0.0036 d^2 - 0.000012 d^3 + 0.0068 r_1 d + \\ &0.0049 r_2 d + (15 + 0.78 d) \tanh(0.41 d). \end{aligned} \tag{13}$$

The coefficient inside the hyperbolic tangent function is not part of the regression but set constant based on a previous optimization using only the hyperbolic tangent components. The expression in Equation (13) had a root mean squared error (RMSE) of 8.3 minutes and a mean percentage error (MPE) of 14 % in the Mapbox dataset. As shown in Figure 1, the hyperbolic tangent is key to capture the relationship between distance and travel time.

D. Cost of Connection to Electricity Grid

The cost of connecting the vertiport and its charging station to the power grid is modeled with the method proposed by

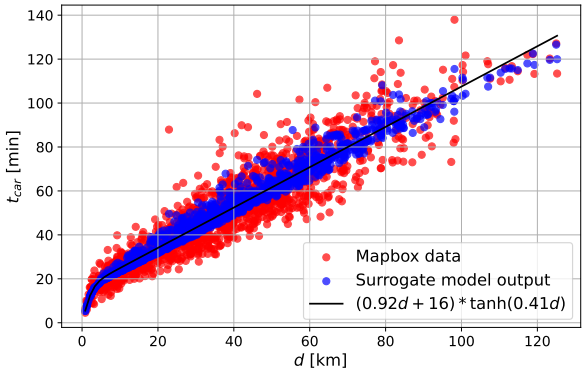

Figure 1. t_{car} against trip distance.

Cintrano et al. [19] for charging stations for cars. The cost of connection is modeled as a linear function of the distance to the nearest electrical substation based on current substation capacity maps [20]. Substations with a spare capacity below 1 [MW] would require an upgrade, which should also be taken into account. This results in Equation (14),

$$\mathrm{CON}_k = \min(d_{ik}c_c + c_u), \quad \forall k \in N. \tag{14}$$

Where d_{ki} is the distance between vertiport k and substation i, c_i is the upgrade cost of substation i, and c_c is the cost per [km] of the cabling, which we assume to be constant.

E. Cost of Urban Floor

To estimate the cost of purchasing urban floor for the construction of a vertiport, we combine price data from unused parcels provided by the Ministerio de Vivienda y Agenda urbana (MIVAU) [21] and price data of apartments from Idealista [22] using a weighted average based on the population density ρ of the district or municipality.

$$C_{land} = \lambda(\rho)C_{apt} + (1 - \lambda(\rho))C_{parcel} \tag{15}$$

Where C_{land} is the resulting land price in [EUR / m^2], C_{apt} is the apartment floor price, C_{parcel} is the unused land price and λ is the mixing factor as a function of population density ρ [people / km^2]:

$$\lambda(\rho) = \max(0, min(1, (\rho - 1500)/2500) \tag{16}$$

F. Weather Constraints

Daily meteorological data from 2022-2024 was extracted from the website of the Agencia Estatal de Meteorologia (AEMET) [23], with information on minimum, maximum and average daily temperatures, maximum average wind speed in a 10 minute interval, and precipitation. For visibility data we used the Automated Surface Observing System (ASOS) website [24]. We map the visibility data onto the AEMET stations based on proximity. After that, for each day the meteorological data and drone specifications are compared to determine whether the drone can operate that day on that meteorological station. This is done with all the daily data available for all stations, which yields the fraction of suitable days for drone A in each station w_A. The data is then linearly interpolated in space to find the values at the vertiport locations. The value used in the optimization is then the minimum out of the access and egress vertiports

$$w_{A,kd} = \min(w_{A,k}, w_{A,d}). \tag{17}$$

G. Code Implementation

The vertiport location optimization tool has been coded entirely using the *python* programming language. The optimization module uses the *pyomo* library [25] to define the objective function and constraints. For the mixed integer linear programming solver, we use the open-source solver SCIP [26].

H. Test Matrix

To test the vertiport optimization tool in a wide variety of scenarios we design a test matrix which we also use to perform a sensitivity analysis of model to the user inputs. The test matrix uses a factorial design, therefore testing all the possible combinations of the selected variable values, which are presented in Table II.

The different drones do not only impact the optimization due to their specifications, but also due to how they modify the requirements for the vertihub. These drones are based on existing designs, but their names are changed. The parameters that are affected and the relevant drone specifications are compared in Table III. Some key differences are the cruise speeds and the area needed for the vertiports. The values for the parameters related to the vertiport and vertihub were extracted from the vertiport sizing tool developed in the MAIA project [27].

TABLE II. TEST MATRIX FOR THE SENSITIVITY ANALYSIS OF THE VERTIPORT OPTIMIZATION TOOL IN THE MADRID CASE STUDY

Variable	Values
eVTOL	Multicopter, Winged eVTOL
n_{vert}[-]	5, 10
TTRP [-]	0.4, 0.7
k_{max} [%]	1, 3, 6, 10, 20
c_{prices} [-]	0.5, 1, 1.5, 2, 4

We have selected 3 different adoption scenarios with $n_{vert} = 10$ and TTRP $= 0.7$:

- 1. Early scenario (Multicopter and Winged): $k_{max} = 3$ [%], $c_{prices} = 1.5$. A lower demand scenario that is more representative of what could be expected initially due to skepticism towards the technology. Higher pricing would be required for the service to be profitable.
- 2. Baseline scenario (Winged): $k_{max} = 6$ [%], $c_{prices} = 1.5$. Meant to represent the demand a few years after the successful introduction of the service.
- 3. Optimistic future scenario (Winged): $k_{max} = 10$ [%], $c_{prices} = 2$. A scenario simulating the demand for the service after over 10 years of successful operations.

TABLE III. VALUES OF THE MODEL PARAMETERS USED FOR THE SENSITIVITY ANALYSIS AND ADOPTION SCENARIOS

	Multicopter	Winged eVTOL
Drone Specifications		
Maximum Dimension [m]	5	12
v_a [km/h]	100	200
Battery Capacity [kWh]	200	300
Range [km]	100	169
$n_{A,pass}$	1	3
Vertiports		
S_v [m^2]	600	3456
INF$_v$ [EUR]	608000	837000
C_v [Operations / day]	23.3	17.6
Vertihubs		
S_h [m^2]	600	3456
INF$_h$ [EUR]	1728000	1957000
C_h [Operations / day]	35.0	26.4

For reference, in the investigated region, 100 [%] of the market would be approximately 34600 trips per day. The remaining model parameters were kept constant using the values specified in Table IV.

IV. Results

The summarized optimization results of the scenarios defined in Section III-H are presented in Table V.

All the scenarios result in a positive profit for the vertiport operator except for Scenario 1 with the Winged eVTOL, with the equivalent for the Multicopter resulting in a net positive. Comparing these, it can be noticed that the Multicopter network produces a significantly higher income per passenger with the pricing scheme we are using for this exercise. This combined with the higher costs due to the larger vertiport needed for the Winged eVTOL results in a significantly lower net revenue, despite capturing more passengers.

Figures 2, 3, and 4 show the selected locations for each of these cases. In all scenarios, the selected locations are relatively close to the center of Madrid, which is the largest city in the investigated area. The capability of eVTOLs to avoid traffic congestion can partly explain these results, as the average speed of a car is lower in this area. However, we assume that the eVTOL will travel at its cruise speed over these urban areas, which may not be the case in the future due to regulations.

It can also be observed in 4 that due to the higher potential demand, one of the vertiports in the city center is upgraded to a vertihub to allow for more passengers. However, the locations themselves are not significantly affected, with 8 of them remaining the same as for Scenario 1 with the Winged eVTOL. For the Multicopter, the results do differ noticeably, with more vertiports being placed in the center of the city. This is likely due to the smaller surface area of the vertiports, which reduces the cost of constructing vertiports in densely populated areas.

TABLE IV. Values of the constant model parameters used for the sensitivity analysis and adoption scenarios

Parameter	Value	Parameter	Value
t_{delay} [min]	6	f_{op} [EUR]	50
$n_{emp,v}$ [-]	10	f_{pass} [EUR / passenger]	25
$n_{emp,h}$ [-]	20	f_e [%]	400
SAL [EUR / year]	24000	MAI_v [EUR / year]	30000
MAI_h [EUR / year]	60000	c_c [EUR/km]	190000
c_u [EUR]	200000	T_a [years]	30

TABLE V. Summary of the optimization results of the selected scenarios

Scenario	Profit [EUR/day]	Income [EUR/day]	Costs [EUR/day]	Passengers [-]	Income per passenger [EUR]
1 - Multi	1410	11600	10200	84	138
1 - Winged	-6420	8480	14900	112	75.7
2 - Winged	1300	17700	16400	234	75.6
3 - Winged	13900	33400	19500	330	101

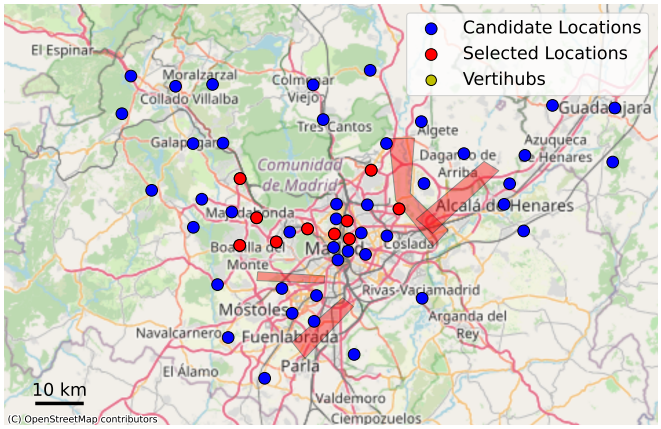

Figure 2. Selected locations for Scenario 1 with Multicopter.

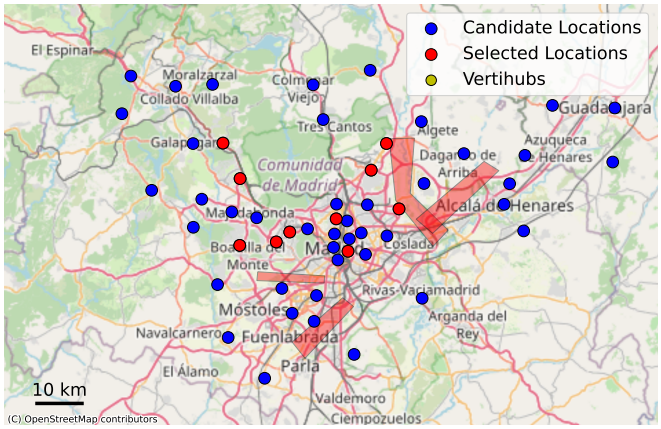

Figure 3. Selected locations for Scenario 1 with Winged eVTOL.

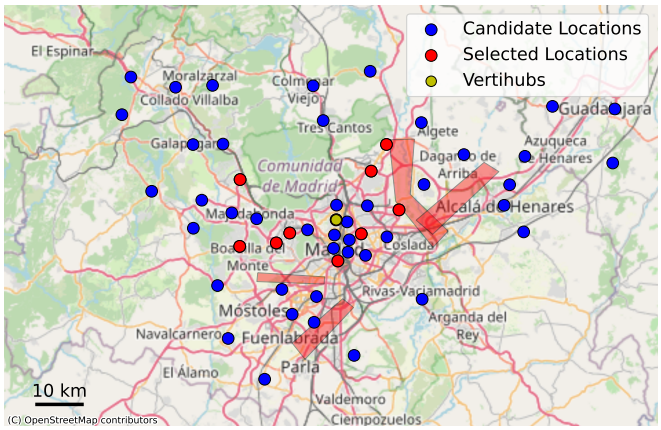

Figure 4. Selected locations for Scenario 2 with Winged eVTOL.

A. Sensitivity Analysis

To better understand the effect of user inputs on the optimization outputs, we completed the simulations of the 200 scenarios based on Table II. In Figure 5 below, the profit is plotted as a function of the maximum market penetration and the pricing multiplier c_{prices}. The resulting contours showcase

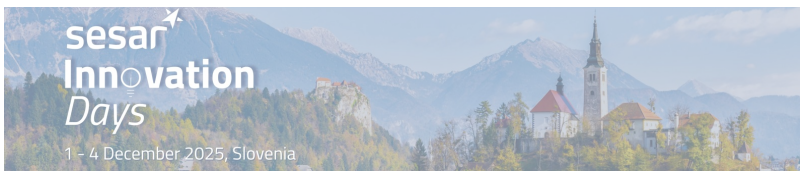

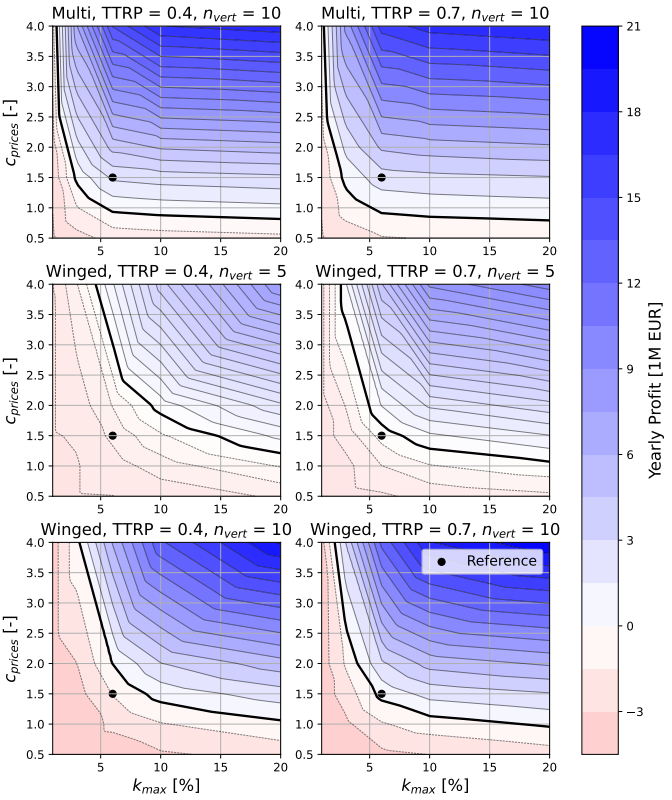

Figure 5. Sensitivity analysis of the yearly profit. The reference point marks the values of c_{prices} and k_{max} of the baseline scenario.

the different possible profit scenarios depending on the level of user adoption, with scenarios becoming more optimistic towards the top right of the graphs. Observing the 0 profit contour lines, it can be noticed that the contour has an asymptotic shape, showing that there is a minimum pricing below which the operation of vertiports cannot be profitable independently of the potential demand, since the vertiports have a limited capacity.

Comparing the four top graphs to the four bottom graphs, it can be noticed that the Multicopter is profitable in significantly more scenarios, as the positive area of the graphs is greater. This agrees with the comparison of Scenario 1 in Table V. Furthermore, the positive area, as well as the profits in the most optimistic scenarios, increases noticeably when using n_{vert} = 10, compared to 5. This is likely due to the number of available routes between vertiports scaling quadratically with N, while the costs for the operator increase linearly with N. Finally, it can be observed that TTRP has a very limited effect on the Multicopter scenarios, as the 0 profit line remains unchanged. However, the effect on the Winged eVTOL scenarios is quite noticeable. This is likely due to the higher cruise speed of the Winged eVTOL (200 [km/h]), which means that it has a great advantage over cars even for longer trips, while the Multicopter (100 [km/h]) only provides a small speed advantage over cars for longer displacements.

Despite the Multicopter producing larger profits, and being profitable for more scenarios, the number of passengers its

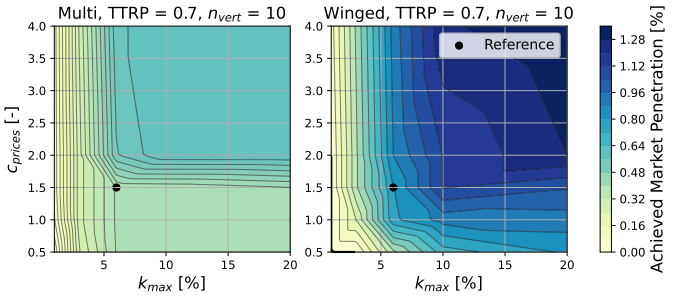

Figure 6. Sensitivity analysis of the number of passengers. The reference point marks the values of c_{prices} and k_{max} of the baseline scenario.

network accommodates is significantly lower. This can be observed in Figure 6. The Multicopter network for the plotted scenarios becomes saturated at $k_{max} \approx 7$ [%], while the network for the Winged eVTOL does not become saturated even at $k_{max} = 20$ [%]. Furthermore, it can also be noticed that the saturated capacity is greater for the Multicopter network when $c_{prices} > 2$, as below that vertihubs are not profitable.

Since the main objective of the tool is to select the locations, we also investigate the sensitivity of the selected network to model parameters. For this we solve the minimum cost assignment problem to minimize total distance between two sets of selected locations. We use the set of selected locations of a reference scenario $R = \{r_1, r_2, ...\}$ and other set of locations $O = \{o_1, o_2, ...\}$, and we find the set of matching pairs $\mathcal{M}$ such that the mean distance between location pairs is minimized,

$$d_{mean} = \frac{1}{n_{vert}} \sum_{(i,j)\in\mathcal{M}} \text{dist}(r_i, o_j). \tag{18}$$

Where dist() is an operator for the Euclidean distance in [km] between the points. Equal sets of locations will have $d_{mean} = 0$. As the selected locations differ more, d_{mean} will increase. Figure 7 shows the value of d_{mean} for the scenarios with $n_{vert} = 10$ using as reference Scenario 2 for the Winged eVTOL, and the equivalent scenario for the Multicopter.

Looking at Figure 7, it can be observed that d_{mean} has very large values for cases with low k_{max}. This is caused by the resulting demand being too low for any vertiport to be profitable, resulting in the model selecting locations with little or no demand, but that are have lower floor costs, thus reducing the losses. Furthermore, at $k_{max} = 20$ [%] the selected locations also differ noticeably from the reference location. This is caused by the demand being high enough that many vertihubs become saturated. This again leads the model towards locations with lower floor costs even if they have a lower demand, since they are still going to be operating near their maximum capacity. Therefore, the locations are more sensitive to the assumed potential demand in the form of k_{max} than to the pricing.

V. Conclusion

In this work, we have presented a tool for the optimization of vertiport locations for passenger transportation. The problem is mathematically framed as an HLP, with the objective function of maximizing the vertiport operator's profit. We approximate the demand for air taxis based on the demand for taxis, estimated through the use of MND OD matrices. Travel time by car is modeled using a surrogate model for a navigation routing system, allowing for better estimates than assuming the same average speed for all OD pairs. We also include costs which directly affect the feasibility of this service, such as the cost of connecting the charging stations to the power grid, as well as the floor costs and the operational costs of the vertiport. Furthermore, we also use daily meteorological data and drone specifications, to take into account lost demand due to poor weather conditions. Access from the origin to the departure vertiport and egress from the arrival vertiport to the destination is considered as extra travel time for the eVTOL trip. Future research should include the variations within a day of car travel time, which highly depend on road congestion and may result in peaks when a higher number of people switch to UAM. A factor that directly impacts capacity, an total eVTOL travel time.

The tool is tested in a case study in the province of Madrid, Spain. A conservative scenario with limited adoption of the technology (maximum possible 3 % market penetration on road taxi demand) by potential users predicts losses when using a large eVTOL with horizontal cruise capabilities, while the equivalent scenario is profitable for a smaller Multicopter eVTOL. A sensitivity analysis of the model showed that the selected locations are similar for moderate levels of adoption, but can change significantly in very low or very high adoption scenarios. Future work will focus on including demand elasticity to price in the model through a discrete choice model based on an intended use poll data. This discrete choice model could be used to include other powerful factors in modal choice, such as reliability, safety perception, privacy, access time, or predictability. Finally, broadening the study to additional areas will aid in generalizing the methodology and findings.

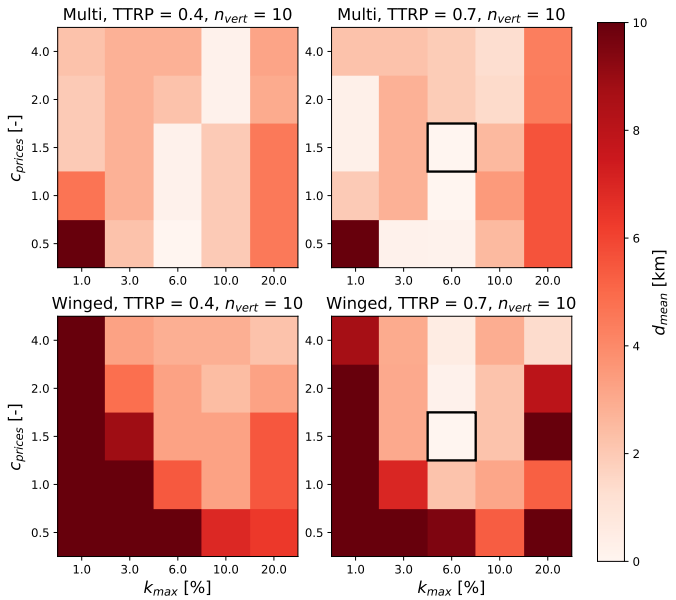

Figure 7. Heat map showing the d_{mean} values for the 100 scenarios with $n_{vert} = 10$. The reference scenarios are outlined in black.

Acknowledgment

This research is part of the SESAR ENGAGE 2 Catalyst funds project "Decision support tool for vertiport site selection". The project is supported by the SESAR 3 Joint Undertaking and its founding members under the Grant Agreement nr. 101114648.

References

[1] L. A. Garrow, B. J. German, and C. E. Leonard, "Urban air mobility: A comprehensive review and comparative analysis with autonomous and electric ground transportation for informing future research," *Transportation Research Part C: Emerging Technologies*, vol. 132, p. 103377, 2021.

[2] K. Schweiger and L. Preis, "Urban air mobility: Systematic review of scientific publications and regulations for vertiport design and operations," *Drones*, vol. 6, no. 7, p. 179, 2022.

[3] U. Elevate, "Fast forwarding to a future of on-demand urban air transportation (2016)," 2016.

[4] N. EASA, "Study on the societal acceptance of urban air mobility in europe," *European Union Aviation Safety Agency and McKinsey & Company*, 2021.

[5] M. Brunelli, C. C. Ditta, and M. N. Postorino, "New infrastructures for urban air mobility systems: A systematic review on vertiport location and capacity," *Journal of Air Transport Management*, vol. 112, p. 102460, 2023.

[6] M. Rimjha, S. Hotle, A. Trani, and N. Hinze, "Commuter demand estimation and feasibility assessment for urban air mobility in northern california," *Transportation Research Part A: Policy and Practice*, vol. 148, pp. 506–524, 2021.

[7] N. Venkatesh, A. P. Payan, C. Y. Justin, E. Kee, and D. Mavris, "Optimal siting of sub-urban air mobility (suam) ground architectures using network flow formulation," in *AIAA AVIATION 2020 FORUM*, 2020, p. 2921.

[8] B. Rahman, R. Bridgelall, M. F. Habib, and D. Motuba, "Integrating urban air mobility into a public transit system: a gis-based approach to identify candidate locations for vertiports," *Vehicles*, vol. 5, no. 4, pp. 1803–1817, 2023.

[9] R. Church and C. R. Velle, "The maximal covering location problem," *Papers in regional science*, vol. 32, no. 1, pp. 101–118, 1974.

[10] S. Rath and J. Y. Chow, "Air taxi skyport location problem with single-allocation choice-constrained elastic demand for airport access," *Journal of Air Transport Management*, vol. 105, p. 102294, 2022.

[11] Z. Jin, K. K. Ng, and C. Zhang, "Robust optimisation for vertiport location problem considering travel mode choice behaviour in urban air mobility systems," *Journal of the Air Transport Research Society*, vol. 2, p. 100006, 2024.

[12] R. Z. Farahani, M. Hekmatfar, A. B. Arabani, and E. Nikbakhsh, "Hub location problems: A review of models, classification, solution techniques, and applications," *Computers & industrial engineering*, vol. 64, no. 4, pp. 1096–1109, 2013.

[13] Z. Wu and Y. Zhang, "Integrated network design and demand forecast for on-demand urban air mobility," *Engineering*, vol. 7, no. 4, pp. 473–487, 2021.

[14] "Open data movilidad — ministerio de transportes, movilidad y agenda urbana," https://www.transportes.gob.es/ministerio/proyectos-singulares/estudios-de-movilidad-con-big-data/opendata-movilidad, Ministerio de Transportes, Movilidad y Agenda Urbana, 2025, accessed: 2025-09-26.

[15] "Edm2018 — enlaces y documentación (crtm)," https://www.crtm.es/conocenos/enlaces-y-documentacion/edm2018/, Consorcio Regional de Transportes de Madrid (CRTM), 2025, accessed: 2025-09-26.

[16] P. E. Hart, N. J. Nilsson, and B. Raphael, "A formal basis for the heuristic determination of minimum cost paths," *IEEE transactions on Systems Science and Cybernetics*, vol. 4, no. 2, pp. 100–107, 1968.

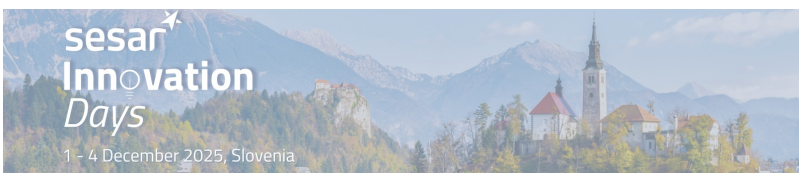

[17] "Mapbox directions api documentation," https://docs.mapbox.com/api/navigation/directions/, Mapbox, 2025, accessed: 2025-09-26.
[18] M. Schmelzer, R. P. Dwight, and P. Cinnella, "Discovery of algebraic reynolds-stress models using sparse symbolic regression," *Flow, Turbulence and Combustion*, vol. 104, no. 2, pp. 579–603, 2020.
[19] C. Cintrano and J. Toutouh, "Multiobjective electric vehicle charging station locations in a city scale area: malaga study case," in *International Conference on the Applications of Evolutionary Computation (Part of EvoStar)*. Springer, 2022, pp. 584–600.
[20] "Mapa de capacidad i-de (30 enero 2025)," https://www.i-de.es/documents/1951486/4922361/MapaDeCapacidad_iDE_30_Enero_2025.pdf/84257ee7-656f-6c57-0396-6c1285d878f4?t=1738243563396, i-DE, 2025, accessed: 2025-09-26.
[21] "Precios de suelo urbano," https://www.mivau.gob.es/el-ministerio/observatorios-y-estadisticas/estadisticas/precios-suelo-urbano, Ministerio de Vivienda y Agenda Urbana (MIVAU), 2025, accessed: 2025-09-26.
[22] "Informes precio vivienda — idealista," https://www.idealista.com/sala-de-prensa/informes-precio-vivienda/venta/madrid-comunidad/madrid-provincia/madrid/, Idealista, 2025, accessed: 2025-09-26.
[23] "Descarga de datos climáticos — aemet 2013," https://datosclima.es/Aemet2013/DescargaDatos.html, 2025, accessed: 2025-09-26.
[24] "Mesonet asos network (españa) — iowa state university," https://mesonet.agron.iastate.edu/request/download.phtml?network=ES__ASOS, Iowa State University Mesonet, 2025, accessed: 2025-09-26.
[25] M. L. Bynum, G. A. Hackebeil, W. E. Hart, C. D. Laird, B. L. Nicholson, J. D. Siirola, J.-P. Watson, and D. L. Woodruff, *Pyomo–optimization modeling in python*, 3rd ed. Springer Science & Business Media, 2021, vol. 67.
[26] S. Bolusani *et al.*, "The SCIP Optimization Suite 9.0," Optimization Online, Technical Report, February 2024. [Online]. Available: https://optimization-online.org/2024/02/the-scip-optimization-suite-9-0/
[27] MAIA Project, "D5.2 maia-uam exploratory research report," MAIA, Tech. Rep., 2025, accessed: 2025-09-26. [Online]. Available: http://vsctool.sf.bg.ac.rs/index.html